Chirp Dependence of Wave Packet Motion in Oxazine 1

Stephan Malkmus, Regina Dürr, Constanze Sobotta, Horst Pulvermacher, Wolfgang Zinth, and Markus Braun*

Department für Physik, Ludwig-Maximilians-Universität, Oettingenstrasse 67, D-80538 München, Germany

Received: August 10, 2005

The motion of vibrational wave packets in the system oxazine 1 in methanol is investigated by spectrally resolved transient absorption spectroscopy. The spectral properties of the probe pulse from 600 to 700 nm were chosen to cover the overlap region where ground-state bleach and stimulated emission signals are detected. The spectral phase of the pump pulse was manipulated by a liquid crystal display based pulse-shaping setup. Chirped excitation pulses of negative and positive chirp can be used to excite vibrational modes predominately in the ground or excited state, respectively. To distinguish the observed wave packets in oxazine 1 moving in the ground or excited state, spectrally resolved transient absorption experiments are performed for various values of the linear chirp of the pump pulses. The amplitudes of the wave packet motion show an asymmetric behavior with an optimum signal for a negative chirp of -0.75 ± 0.2 fs/nm, which indicates that predominantly ground-state wave packets are observed.

Introduction

Optical pump−probe spectroscopy allows for transient absorption experiments with the highest temporal resolution in the femtosecond time regime. This technique helps to elucidate the fastest fundamental processes in photochemistry and photobiology like isomerization, electron transfer, and proton transfer. Broad-band optical parametric amplifiers operating according to the NOPA (noncollinear optical parametric amplifier) principle deliver tunable pulses in the UV/vis to NIR range that can be compressed to about 10 fs or even below.[1−3] Nowadays light pulses are short enough to facilitate studies of molecular vibrations in real time by the observation of vibrational wave packets via transient absorption spectroscopy in the visible spectral range.[4−7] Therewith the fingerprint region of organic and biological relevant molecules in the frequency range of up to 2000 cm^{-1} is accessible.[8−10]

The generation of excited-state vibrational wave packets (a coherent superposition of vibrational states) in a molecular system by an ultrashort laser pulse has been treated by many authors.[4−7,11−14] It relies on the fact that the minimum of the excited-state potential energy surface is displaced along a nuclear coordinate with respect to the minimum of the ground-state potential energy surface. This is the result of the different equilibrium geometries of a molecule in the electronic ground or excited state due to changed electron distributions. Therefore, the excitation of a molecule in the Franck−Condon region using an ultrashort laser pulse prepares the molecules not at the equilibrium position of the excited electronic state. This state can be regarded as a superposition of vibrational modes. The vibrational wave packet in the excited state starts to evolve along the gradient to the minimum of the excited-state potential energy surface. In the harmonic approximation for the potential energy surface the excited-state vibrational wave packet oscillates with different vibrational eigenmodes. If the exciting laser pulse is shorter in time than the period of a vibration, this oscillation can be observed via a modulation of the optical properties connected to the electronic excited state. This would be for example the induced absorption, stimulated emission, or spontaneous emission signals.

The generation of a vibrational wave packet in the electronic ground state is a little more complex. It is described by a Raman-like interaction of the excitation pulse with the molecule that leads to a coherent motion of a wave packet in the electronic ground state.[11−14] In this case the optical transitions originating from the electronic ground state can be used to probe this kind of vibrational wave packet. The ground-state wave packet can therefore be observed e.g. as a modulation of the ground-state absorption signal.

If a molecular system is excited by an ultrashort laser pulse, both vibrational wave packets in the electronic ground state and the electronic excited state may be generated simultaneously. Therefore, a separation and classification of the observed vibrations to both states is necessary. Unfortunately, often the spectral regions with optical signals connected to ground- and excited-state wave packets are not separated. This complicates an unambiguous assignment of the vibrational spectrum to ground- or excited-state motions. Especially for molecular systems with a small Stokes shift the absorption and emission spectra overlap and a simple assignment of observed modes by the probe wavelength is not possible.

This problem can be solved by a method that uses excitation pulses with linear positive and negative chirps. This method was introduced by Bardeen et al.[14] and takes advantage from the different generation schemes of electronic ground-state and excited-state wave packets. For the optimal preparation of a wave packet in the electronic excited state a short optical pulse is needed to generate the desired vibrational coherence. This is achieved by using transform-limited pump pulses. However, the excitation of a ground-state wave packet is usually described by the impulsive resonant Raman process. Here, in a first field interaction the electric field of the excitation pulse generates an amplitude of a wave packet in the excited-state potential energy surface. Here it evolves according to the Hamiltonian of the electronically excited state. Some time later a second field interaction projects the excited-state wave function onto

* Corresponding author. Email: Markus.Braun@physik.uni-muenchen.de; Fax: +49-89/2180-9202.

10.1021/jp054462g CCC: $30.25
Published on Web 10/22/2005

the electronic ground state. It repopulates the electronic ground state with a now displaced vibrational wave packet. As the wave packet on the excited state propagates between the two field interaction processes, i.e., during the pulse duration of the excitation pulse, this process is enhanced if the second field interaction happens with a red-shifted frequency. Therefore, a negatively chirped excitation pulse may improve the generation of the electronic ground-state wave packet. This property allows to discriminate between wave packets in the electronic ground or excited state: for excited-state wave packets an experiment with positively and negatively chirped excitation pulses of identical pulse duration would show no differences, whereas for ground-state wave packets an enhancement should be observed for negatively chirped pulses.

In this study we present transient absorption data on the laser dye oxazine 1[15] in methanol with transform-limited and various linearly chirped excitation pulses. In control experiments on Na_2[16] or I_2[17] using chirped pulses the anharmonicity of the excited state was successfully exploited for reaching the control target. In our case of oxazine 1 the anharmonicity in the excited state should be comparatively low for the investigated vibrations as they are collective ring modes. The chirp of the pump pulse optimizes here the generation of a ground-state wave packet by the impulsive resonant Raman process, and therefore, the anharmonicity of the vibrational mode in the excited state plays a minor role. We use these experiments to assign the wave packets to the electronic ground-state and excited-state potential energy surface. Moreover we vary the linear chirp parameter to determine the optimal pulse for exciting an electronic ground-state wave packet.

Materials and Methods

The laser system for the transient absorption measurements[18,19] consists of a home-built Ti:Sapphire oscillator (100 MHz repetition rate, 20 fs pulse duration, 10 nJ pulse energy) and a regenerative amplifier (1 kHz repetition rate, 80 fs pulse duration, 350 μJ pulse energy) at a central wavelength of 800 nm. The output of the laser is used as a pump source for two single-stage NOPA that deliver pump and probe pulses for the transient absorption measurements in the visible spectral range. By the adequate choice of crystal angle and noncollinear angles for the NOPA process broad (up to 200 nm wide) spectral profiles of the pulses can be achieved. Here the fine-tuning of the NOPA process is optimized to obtain preferably unstructured spectral profiles (see Figure 1b). Therefore, prepulses and afterpulses can be minimized. The center wavelength of the pump pulse is adjusted to 570 nm, and that of the probe pulse to 650 nm. Both pulses are compressed to 13 and 15 fs, respectively, by eliminating the linear component of the spectral chirp in a quartz prism compressor.

The output of one NOPA is split in two parts, a probe pulse and a reference pulse. Both pulses pass the same volume of the sample under an angle of 10°. The reference pulse arrives at the sample prior to the pump and probe pulse. The delay between pump and probe pulse is varied by a mechanical delay stage. The transmitted light of reference and probe pulses is spectrally resolved by a multichannel detection setup that allows for simultaneous acquisition of transient absorption in a wide spectral range with a wavelength resolution of 6 nm. This setup consists of two identical spectrometers and two photodiode arrays (42 elements, each) that are read out with a repetition rate of 1 kHz.

In the experiment the transient absorption signal is recorded as a function of the linear chirp parameter of the pump pulse.

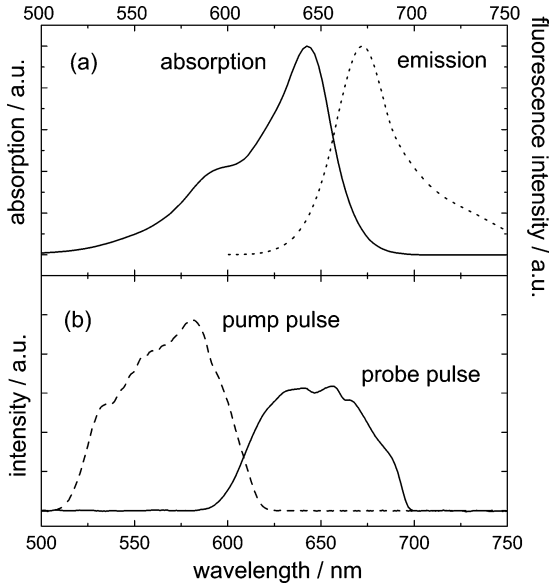

Figure 1. (a) Steady-state absorption and emission spectrum of oxazine 1 dissolved in methanol. (b) Spectra of pump pulse (duration of 13 fs at 570 nm) and probe pulse (duration of 15 fs at 650 nm).

Therefore, the pump pulse is manipulated by a pulse shaping setup[20−22] in a standard 4-f-configuration. To reduce group velocity dispersion reflective optics is used in this setup. The shaper consists of two gratings, two cylindrical silver mirrors, a polarizer, and a spatial light modulator (SLM). For this purpose we use the SLM-256 (CRI, Inc.) that consists of two liquid-crystal (LC) array masks with 128 pixels each. It allows the independent control of spectral shape and spectral phase of the pulse. The gratings of the pulse shaper are chosen to allow for the shaping of 150 nm broad pulses. For our experiments only the spectral phase of the pump pulses is manipulated yielding a linear spectral chirp parameter Φ between -2.0 and 1.0 fs/nm. The application of the SLM pulse shaper allows for a controlled fine scanning of the chirp parameter.

All pulses are characterized by measuring their spectrum, autocorrelation, and cross-correlation FROG (frequency-resolved optical gating). Although the experimental error for the determination of the linear chirp parameter of the pulses by cross-correlation FROG measurements is small, the accuracy of 0.1 fs/nm given here accounts for the remaining chirp of higher orders. The pump pulse with the optimal compensation for the linear chirp parameter that was achievable is referenced as a transform-limited pulse. We used low pulse energy of a few nanojoules for optical excitation. That led to an excitation of well below 10% of the sample in the pumped volume. The excitation density we calculated was about 10^9 W/cm^2. Therefore, we are in the standard regime of low excitation intensities. Furthermore we confirmed the linearity of the transient absorption signal by measuring the intensity dependence.

The laser dye oxazine 1 was purchased by Lambda-Physik and dissolved in methanol (Merck) without further purification. A 10 mL volume of this solution was pumped through a quartz flow cell (thickness 50 μm) to exchange the excitation volume completely after each laser shot. The thin flow cell ensures that no group velocity effects influence the pulse parameter during the excitation and probing process. The concentration of oxazine 1 was chosen to yield an optical transmission of 10% at the absorption maximum at 643 nm in the 50 μm cuvette.

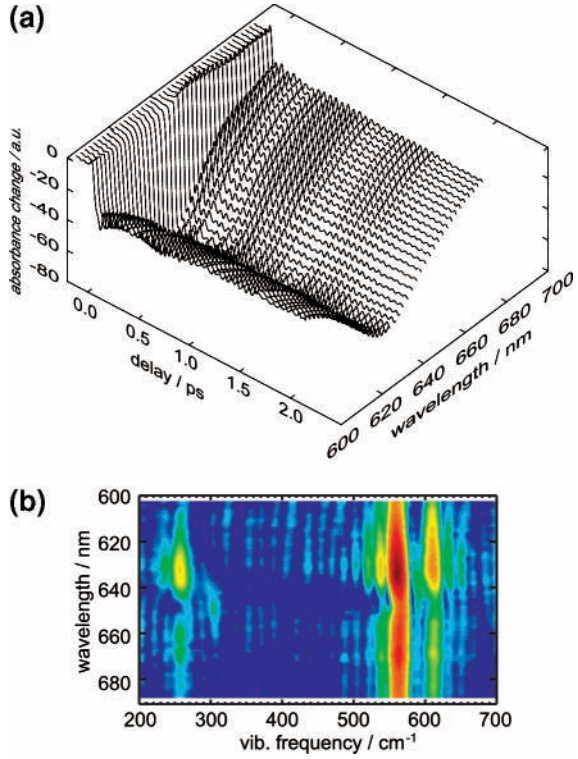

Figure 2. (a) 3-D plot of transient absorption signal as a function of probe wavelength (600−690 nm) and delay time (−0.1 to 2.1 ps). The transient absorption signal exhibits strong modulations with a period of about 60 fs. (b) Fourier transformed data of the time-resolved data shown in (a). The Fourier amplitude (color code) is plotted against the probe wavelength and vibrational frequency. The three dominant modes are located around 260, 560, and 609 cm^{-1}.

Results and Data Evaluation

The steady-state absorption and emission spectrum of oxazine 1 in methanol is presented in Figure 1a. The spectra of pump and probe pulse are shown in Figure 1b. The spectrum of the pump pulse (at 570 nm) remains unchanged also if the linear chirp parameter is varied by the SLM-based pulse shaper. The spectrum of the applied probe pulse covers the overlap region of absorption and fluorescence. Therefore, the transient absorption signals may show contributions from both, ground-state bleaching and stimulated emission.

A typical data set of the transient absorption signal recorded as a function of delay time and probe wavelength is shown in Figure 2a. At zero delay time an immediate negative transient absorption signal (absorption decrease) is observed for all probe wavelengths. This transient absorption signal shows no decay in the chosen delay time range between 0.0 and 2.1 ps of the experiment. However, it is strongly modulated with a period of about 60 fs.

The frequency spectrum of the modulation is obtained by the Fourier transformation (FT) of the modulated signal, as follows. By a standard data treatment the slow population kinetics of the transient absorption signal are subtracted from the measured data set. Then the resulting residuum consists only of the oscillating signal component. This residuum data set is Fourier transformed, and a spectrum of the observed vibrational modes as a function of probe wavelength is obtained, as shown in Figure 2b. The amplitude of the FT data set is presented in a color code. A thorough evaluation for these FT spectra using a semiautomated algorithm which is appropriate also for the analysis of very weak modes will be presented elsewhere.[23] According to DFT-B3LYP calculations using the 6-31G* basis

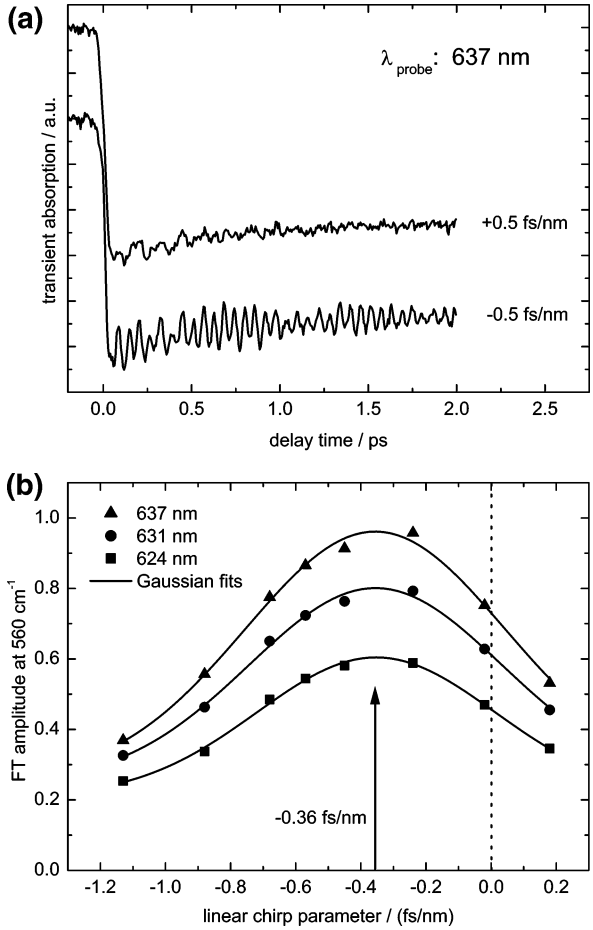

Figure 3. (a) Transient traces recorded for different linear chirp parameters of the pump pulse (probe wavelength: 637 nm). The oscillatory part of the signal is strongly reduced for a positive linear chirp parameter Φ, and the optimum value is found for negative chirps. (b) FT amplitude of the dominant mode at 560 cm^{-1} for different probe wavelengths plotted against Φ. A Gaussian fit (lines) yields a value of Φ_{exp} (fs/nm) for the optimal chirp parameter.

set (not discussed in detail here), the three strongest modes are identified as ring modes: an out-of-plane mode at 260 cm^{-1}; in-plane NO-bending mode at 560 cm^{-1}; in-plane O-bending mode at 609 cm^{-1}. This work concentrates on the strongest modes at 560 and 609 cm^{-1}.

The transient absorption signal was recorded as a function of the probe wavelength and delay time for various linear chirp parameters Φ of the pump pulse. A typical oscillation pattern similar to that seen in Figure 2a was observed on the transient absorption traces for $-1.2 \leq \Phi \leq 0.2$ fs/nm. In Figure 3a the amplitudes of the wave packet oscillation visible in the transient absorption signal are compared for linear chirp values Φ of −0.5 and 0.5 fs/nm. Even without any further data analysis it is obvious that, for the same absolute value of the linear chirp parameter, a negative chirp leads to a higher amplitude of the oscillatory signal component (see Figure 3a). For the quantitative analysis of the vibrational spectra the transient absorption data for each setting of the pump pulse chirp was treated as described above. Qualitatively the FT spectra resemble those for the transform-limited excitation in Figure 2b. Nevertheless the amplitude of the modes in the FT spectrum showed a strong dependence on the linear chirp Φ of the excitation pulse. This is shown for the strongest mode 560 cm^{-1} and various probe wavelengths in Figure 3b. Here, the amplitude of the 560 cm^{-1} mode is plotted against Φ. A fit of the chirp dependence with a Gaussian profile weighting yields the optimal linear chirp

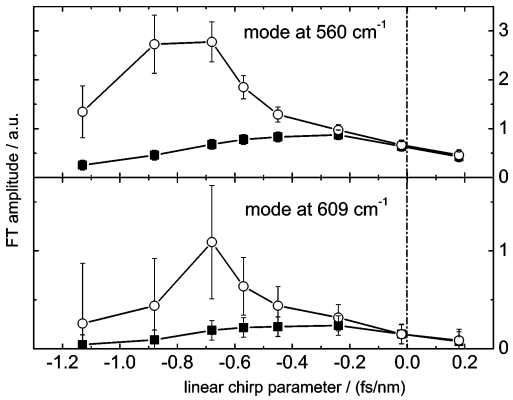

Figure 4. FT amplitude of the modes at (a) 560 cm^{-1} and (b) 609 cm^{-1} as a function of Φ. Data points as squares show the FT amplitude as determined directly from the Fourier transformation (see also Figure 3b). Data points as open circles show the data corrected for the limited temporal resolution (see eq 1). For the modes at 560 and 609 cm^{-1} a linear chirp parameter of about -0.75 ± 0.2 fs/nm is found to be optimal for the excitation of a ground-state wave packet.

parameter $\Phi_{exp} = -0.36 \pm 0.1$ fs/nm. The respective chirp dependence of the mode 609 cm^{-1} is shown in Figure 4.

It should be noted that no dependence of the ground-state or excited-state population on the applied pump pulse chirp was observed. After subtraction of the oscillatory components the transient absorption signal was independent of the pump pulse chirp.

Discussion

The transient absorption experiments with various chirp parameters Φ of the pump pulse described above showed an asymmetric behavior of the wave packet motion as a function of the pump pulse chirp. The FT amplitude of the vibrational mode at 560 cm^{-1} (see Figure 3b) was determined to be strongest when a linear chirp parameter $\Phi_{exp} = -0.36 \pm 0.1$ fs/nm is applied to the pump pulse. In the following this asymmetric behavior will be explained.

At first it should be stated that this asymmetric behavior is not due to higher order chirp effects. For the generation of the linearly chirped excitation pulses a transform-limited pump pulse was manipulated by the SLM pulse-shaping setup as described in Materials and Methods. Only the spectral phase was manipulated by parabolic phase masks. Therefore higher order chirp parameters and the spectrum were not influenced. This was also verified by measuring the autocorrelation and cross correlation FROG traces of pump and probe pulse for each value of the pump pulse chirp.

Mainly, two dominant effects determine the amplitude of a vibrational mode in the FT spectrum, when the chirp Φ of the pump pulse is varied: (i) A linear chirp of either sign increases the pump pulse duration and thus the cross-correlation time of the transient absorption experiment; therefore, the oscillation pattern is smeared out and the FT amplitudes of the vibrational modes are reduced. (ii) As shown above, a negative linear chirp improves the generation of a ground-state wave packet and therefore increases the amplitude of the vibrational mode in the FT spectrum. The combination of both effects leads to an optimum chirp value that represents the compromise between improved ground-state wave packet generation and reduced temporal resolution.

To extract the optimum chirp value Φ_{corr} that is exclusively due to the increased excitation of the ground-state wave packet, the FT data have to be corrected for the influence of a reduced temporal resolution. The effect of a chirped pump and probe pulse on the transient absorption measurement was described quantitatively by Kovalenko et al.[24] In their work the differential optical signal of a pump−probe experiment is calculated from the third-order nonlinear polarization $P^{(3)}(t,\tau)$ of the molecular system. With reference to their notation, this nonlinear polarization can be written as a sum of three components, the so-called sequential term, the Raman term, and the two-photon absorption term. In our case the Raman and two-photon absorption contributions can be neglected, and therefore, the nonlinear polarization according to Kovalenko et al.[24] is written as

$$P^{(3)}(t,\tau) = 2E_2(t-\tau)\int_{-\infty}^{\infty} \mathrm{d}t'\, R_S(t-t')E_1^*(t')E_1(t') \quad (1)$$

where τ is the time delay between pump and probe pulse, $E_1(t)$ is the electric field of the pump pulse, $E_2(t)$ is that of the probe pulse, and $R_S(t)$ is the response function of the molecular system. The interpretation of that formula is straightforward: the response function of the prepared state is the convolution of the original response function $R_S(t)$ and the intensity of the pump pulse.

As vibrational states are studied in this analysis, the fast molecular response function $R_S(t)$ is a cosine function (neglecting the slow dephasing term) and therefore the damping for a cosine function as a function of vibrational frequency and pump pulse chirp has to be calculated. It follows immediately from eq 1 that this damping is simply via the intensity of the pump field $E_1(t)$. This interpretation casts some light on the nature of this approximation: it only describes the trivial reduction of the temporal resolution and therewith the reduction of the FT amplitudes of vibrational modes at high frequencies.

The damping of the vibrational modes was calculated from the measured pump pulse parameters. The measured chirp dependent data (see Figures 3b and 4 (squares)) were then corrected for the temporal resolution as a function of the pump pulse chirp using eq 1. The corrected data set is also shown in Figure 4 (open circles). This data set should be free of temporal resolution effects and represents only the effects of optimal wave packet generation.

For the modes at 560 and 609 cm^{-1} a strong asymmetric behavior with respect to the pump pulse chirp parameter is found. In both cases the measurement yields the same optimal chirp value Φ_{exp} of about -0.36 ± 0.1 fs/nm. After the correction for the temporal resolution according to eq 1 an optimal chirp value Φ_{corr} of about -0.75 ± 0.2 fs/nm is obtained. This negative value of the optimal chirp parameter Φ_{corr} supports the assignment that the investigated oscillations at 560 and 609 cm^{-1} are predominantly due to wave packet motion in the ground state.

In the following we will give an estimate for the linear chirp parameter Φ_{est} of the pump pulse that leads to an optimal oscillatory amplitude in the transient signal due to a wave packet in the ground state. Figure 5 shows a sketch for the different processes leading to wave packet motion on the excited state (Figure 5, left) and the ground state (Figure 5, right). Excitation of the molecule (Figure 5, left) with an ultrashort optical pulse (1) leads to a coherent superposition of the vibrational levels of the excited state, and a wave packet evolves (2) on the excited-state potential energy surface. An optimal wave packet, with the vibrational levels excited in phase, is therefore generated if a transform-limited excitation pulse is applied.

We will focus here on the ground-state wave packet and its generation by the impulsive resonant Raman process (Figure 5, right).[13,14,25,26] A first electric field interaction (1) between

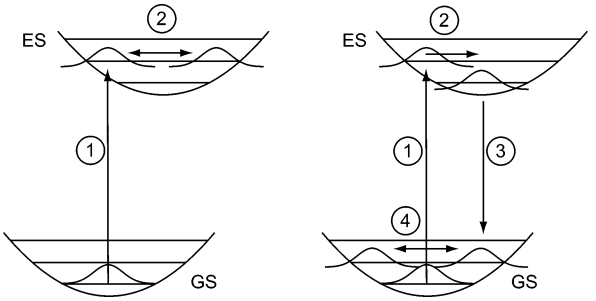

Figure 5. Sketch of the excitation schemes for (left) excited-state wave packets and (right) ground-state wave packets. (For details, see text.)

pump pulse and molecule leads to a coherent polarization between ground and excited state and, therefore, a projection of the ground-state wave function to the excited-state potential energy surface. This wave packet starts to evolve (2) and therefore is displaced from its original position. The second field interaction (3) can project this displaced wave packet back to the ground-state potential energy surface (4). This interaction depends on the separation of the potential energy surfaces at the actual position of the wave packet and the frequency of the second electric field. It should be noted that the second field interaction must not be caused by a second excitation pulse. First and second field interactions may result from temporally separated parts of one light pulse.

Depending on the time delay between the first and second field interaction the resonance energy for this transition may have changed due to the evolution of the wave packet on the excited-state potential energy surface. When chirped excitation pulses are applied for this generation scheme, the frequency shift in the light pulse may deliver the appropriate wavelength at a certain delay time. By this way the wave packet generation may be optimized for the ground state. Therewith the proper time delay between the two field interactions (1 and 3) in combination with the proper frequency shift between the two fields (length of the arrows 1 and 3) will determine the linear chirp of the pump pulse for the optimized preparation of the ground-state wave packet.

We now introduce a simple model to estimate this optimum chirp parameter: After the generation of the excited-state wave packet good projection to a vibrational wave packet in the ground state requires optimum overlap of the vibrational wave functions, which may be accomplished from the center of the S_1 surface (which is reached after a quarter period of the vibrational period). Accordingly the transition frequency of the second electric field should be red-shifted by the vibrational frequency.

For the 560 cm^{-1} mode (vibrational period of 60 fs) the excited-state wave packet has evolved to the minimum of the excited-state parabola after a delay of 15 fs. The difference of the 0−0 transition of oxazine 1 at 642 nm and the 0−1 transition which is 560 cm^{-1} blue-shifted at 620 nm determines approximately the necessary wavelength shift of 22 nm. This corresponds to an optimized negative chirp parameter $\Phi_{est} =$ 15 fs/22 nm, or −0.68 fs/nm. This value agrees well with the measured optimal chirp value Φ_{corr} of -0.75 ± 0.2 fs/nm, determined above. Apparently the observed wave packet should be a ground-state wave packet predominantly generated by an impulsive resonant Raman process.

Conclusion

We presented spectrally resolved transient absorption measurements of oxazine 1 in methanol with 15 fs pulses. By the scanning of the linear chirp parameter of the pump pulse Φ via a pulse shaping setup, the influence of the mere linear chirp on wave packet motion was investigated. This experiment allowed us to identify the potential energy surface where wave packet motion takes place. Due to the asymmetric dependence of the wave packet amplitude regarding the sign of Φ, the observed vibrational modes can be assigned to ground-state wave packets. An optimal value for efficient ground-state wave packet generation was obtained from these experiments. This observation agrees well with theoretical predictions. It is shown that the application of a definite chirp for the pump pulse can populate a definite target state with an optimized wave packet. The generation of a coherent wave packet in the ground state may prove to be an important tool not only for spectroscopic applications but also for the realization of coherent quantum control schemes.

Acknowledgment. We thank A. Peine and P. Gilch for fruitful discussion. This project was funded by the Deutsche Forschungsgemeinschaft (Grant SFB 533).

References and Notes

(1) Baum, P.; Lochbrunner, S.; Riedle, E. *Appl. Phys. B* **2004**, *79*, 1027−1032.

(2) Wilhelm, T.; Piel, J.; Riedle, E. *Opt. Lett.* **1997**, *22*, 1494.

(3) Riedle, E.; Beutter, M.; Lochbrunner, S.; Piel, J.; Schenkl, S.; Sporlein, S.; Zinth, W. *Appl. Phys. B* **2000**, *71*, 457.

(4) Wise, F. W.; Rosker, M. J.; Tang, C. L. *J. Chem. Phys.* **1987**, *86*, 2827.

(5) Garraway, B. M.; Suominen, K. A. *Rep. Prog. Phys.* **1995**, *58*, 365.

(6) Zewail, A. H. *J. Phys. Chem.* **1996**, *100*, 12701.

(7) Bloembergen, N. *Rev. Mod. Phys.* **1999**, *71*, S283.

(8) Gilch, P.; Baigar, E.; Pulvermacher, H.; Zinth, W. Femtosecond wave packet motion and fastest electron-transfer reaction. Presented at the XII UPS Conference, Florence, Italy, 2001.

(9) Lanzani, G.; Zavelani-Rossi, M.; Cerullo, G.; Comoretto, D.; Dellepiane, G. *Phys. Rev. B* **2004**, *69*.

(10) Saito, T.; Kobayashi, T. *Opt. Mater.* **2003**, *21*, 301.

(11) Domcke, W.; Stock, G. Theory of ultrafast nonadiabatic excited-state processes and their spectroscopic detection in real time. In *Advances in Chemical Physics*; Prigogine, I., Rice, S. A., Eds.; John Wiley & Sons: New York, 1997; Vol. 100.

(12) Hasche, T.; Ashworth, S. H.; Riedle, E.; Woerner, M.; Elsaesser, T. *Chem. Phys. Lett.* **1995**, *244*, 164.

(13) Pollard, W. T.; Lee, S. Y.; Mathies, R. A. *J. Chem. Phys.* **1990**, *92*, 4012.

(14) Bardeen, C. J.; Wang, Q.; Shank, C. V. *Phys. Rev. Lett.* **1995**, *75*, 3410.

(15) Yoshihara, K.; Tominaga, K.; Nagasawa, Y. *Bull. Chem. Soc. Jpn.* **1995**, *68*, 696.

(16) Assion, A.; Baumert, T.; Helbing, J.; Seyfried, V.; Gerber, G. *Chem. Phys. Lett.* **1996**, *259*, 488.

(17) Kohler, B.; Yakovlev, V. V.; Che, J. W.; Krause, J. L.; Messina, M.; Wilson, K. R.; Schwentner, N.; Whitnell, R. M.; Yan, Y. J. *Phys. Rev. Lett.* **1995**, *74*, 3360.

(18) Engleitner, S.; Seel, M.; Zinth, W. *J. Phys. Chem. A* **1999**, *103*, 3013.

(19) Baigar, E.; Braun, M.; Peine, A.; Konjaev, V.; Zinth, W. Convenient tunability of sub-10 fs-pulses in the visible range. Presented at Ultrafast Phenomena, Vancouver, Cananda, 2002.

(20) Brixner, T.; Gerber, G. *ChemPhysChem* **2003**, *4*, 418.

(21) Weiner, A. M. *Rev. Sci. Instrum.* **2000**, *71*, 1929.

(22) Wohlleben, W.; Degert, J.; Monmayrant, A.; Chatel, B.; Motzkus, M.; Girard, B. *Appl. Phys. B* **2004**, *79*, 435.

(23) Braun, M.; Malkmus, S.; Sobotta, C.; Dürr, R.; Pulvermacher, H.; Zinth, W., to be submitted for publication.

(24) Kovalenko, S. A.; Dobryakov, A. L.; Ruthmann, J.; Ernsting, N. P. *Phys. Rev. A* **1999**, *59*, 2369.

(25) Bardeen, C. J.; Wang, Q.; Shank, C. V. *J. Phys. Chem. A* **1998**, *102*, 2759.

(26) Ruhman, S.; Kosloff, R. *J. Opt. Soc. Am. B* **1990**, *7*, 1748.